PART II

IMAGING OF VESSEL WALL FUNCTION

CHAPTER 4

EVALUATION OF SAMPLING DENSITY ON THE ACCURACY OF AORTIC PULSE WAVE VELOCITY FROM VELOCITY-ENCODED MRI IN PATIENTS WITH MARFAN SYNDROME

E.S.J. Kröner, R.J. van der Geest, A.J.H.A. Scholte, L.J.M. Kroft, P.J. van den Boogaard, H.J. Lamb, H.J. Siebelink, B.J.M. Mulder, M. Groenink, T. Radonic, Y. Hilhorst-Hofstee, J.J. Bax, E.E. van der Wall, A. de Roos, J.H.C. Reiber, J.J.M. Westenberg

J Magn Reson Imaging 2012;36:1470-6.

ABSTRACT

Purpose: To evaluate the effect of spatial (i.e. number of sampling locations along the aorta) and temporal sampling density on aortic Pulse Wave Velocity (PWV)-assessment from velocity-encoded MRI in patients with Marfan syndrome (MFS).

Methods: Twenty-three MFS patients (12 men, mean age 36±14 years) were included. Three PWV-methods were evaluated: (1) reference $PWV_{i.p.}$ from in-plane velocity-encoded MRI with dense temporal and spatial sampling; (2) conventional $PWV_{t.p.}$ from through-plane velocity-encoded MRI with dense temporal but sparse spatial sampling at three aortic locations; (3) EPI-accelerated $PWV_{t.p.}$ with sparse temporal but improved spatial sampling at five aortic locations with acceleration by echo-planar-imaging (EPI).

Results: Despite inferior temporal resolution, EPI-accelerated $PWV_{t.p.}$ showed stronger correlation (r=0.92 versus r=0.65, p=0.03) with reference $PWV_{i.p.}$ in the total aorta, with less error (8% versus 16%) and variation (11% versus 27%) as compared to conventional $PWV_{t.p.}$. In the aortic arch, correlation was comparable for both EPI-accelerated and conventional $PWV_{t.p.}$ with reference $PWV_{i.p.}$ (r=0.66 versus r=0.67, p=0.46), albeit 92% scan-time reduction by EPI-acceleration.

Conclusions: Improving spatial sampling density by adding two acquisition planes along the aorta results in more accurate PWV-assessment, even when temporal resolution decreases. For regional PWV-assessment in the aortic arch, EPI-accelerated and conventional PWV-assessment are comparable accurate. Scan-time reduction makes EPI-accelerated PWV-assessment the preferred method-of-choice.

INTRODUCTION

Patients with Marfan syndrome (MFS) have a genetic mutation in the fibrillin-1 gene resulting in increased regional aortic wall stiffening and aortic dilatation (1). Indices of aortic stiffness are prognostically important in MFS patients (2). A surrogate marker of aortic stiffness is aortic Pulse Wave Velocity (PWV), defined as the propagation speed of the systolic velocity wave front through the aorta (3). PWV is a strong predictor of future cardiovascular events and all-cause mortality (4). In MFS patients, PWV assessment is performed in clinical trials that investigated the efficacy of several drugs to attenuate arterial stiffness (5,6). Because of regional variability in aortic wall stiffening in MFS, both global and regional PWV assessment are of clinical importance (7).

Recently, it was shown that dense temporal and spatial PWV-sampling by two-directional in-plane VE MRI covering the whole aorta in a multi-slice 3-plane volume scan (i.e., $PWV_{i.p}$) is the most accurate approach for aortic PWV-assessment with MRI, as it showed high agreement with invasive pressure measurements (8). However, this dense sampling strategy is time-consuming, which is paramount for clinical application. Therefore, one-directional through-plane VE MRI-acquisitions at two locations along the aorta (i.e. $PWV_{t.p}$) (9) is conventionally performed. Sampling with sparse spatial density is considered to represent aortic PWV less accurately as reported correlation with the gold standard was only moderate (9). To ensure adequate temporal resolution – crucial for accurate definition of the transit-time (i.e. the time duration for systolic flow wave to travel between acquisition sites, which defines the PWV) – usually a non-segmented single-readout technique with a relatively long scan time is applied. This long scan time also limits the application of respiratory motion compensation. Accelerating the acquisition by using multiple readouts per echo (e.g. by echo-planar imaging, EPI) will reduce acquisition time and may enable breath-holding. Furthermore, reduction of total acquisition time will enable improvement in spatial sampling density by adding multiple acquisition planes along the aorta within the available examination time. However, this reduction in acquisition time comes at a penalty regarding temporal sampling resolution, as the repetition time will increase with the multiple readouts per echo.

Importantly, the effect of temporal and spatial sampling density on the accuracy of aortic PWV-assessment in patients with MFS remains to be investigated. Therefore, the purpose of this study was to compare conventional $PWV_{t.p.}$ to EPI-accelerated $PWV_{t.p.}$ against the reference $PWV_{i.p.}$, both for the total aorta and for the regional PWV assessment in the aortic arch. This study introduces PWV-assessment with sparse temporal but improved spatial sampling by four EPI-accelerated one-directional through-plane VE MRI acquisitions along the aorta, which results in accelerated $PWV_{t.p}$-sampling at five aortic locations. Of note, the acquisition plane at the level of the pulmonary trunk transects both the ascending aorta and the proximal descending aorta, providing two aortic sampling locations.

MATERIAL AND METHODS

Patient population and study protocol

Twenty-three patients (12 men, 11 women, mean age 36±14 years) with MFS diagnosed according to the Ghent criteria (10), were included. None of these patients had undergone aortic surgery. Patients temporarily refrained from beta-adrenergic blocking medication and were at least 24 hours without medication prior to MRI. All patients gave informed consent and approval from the local Medical Ethical Committee was obtained. Part of the data of this patient group has been published before in a study focusing on age-related PWV (7).

All patients underwent three methods for PWV-assessment by VE MRI; (1) conventional $PWV_{t.p}$ at three aortic locations; (2) EPI-accelerated $PWV_{t.p}$ at five aortic locations; (3) reference $PWV_{i.p.}$ covering the full aorta. In Figure 1, a schematic representation of the three PWV-methods is presented.

MRI acquisition

MRI was performed using a 1.5T scanner (Intera, release 12; Philips Medical Systems, Best, the Netherlands). Imaging sequences were previously described (8). In short, after acquisition of a series of thoracic survey images, a three-slice volume slab (covering a para-sagittal view of the aorta) was obtained with a steady-state free precession (SSFP) sequence and used for planning (8). Aortic PWV was subsequently assessed with two one-directional through-plane VE MRI (conventional $PWV_{t.p.}$), four accelerated one-directional through-plane VE MRI (EPI-accelerated $PWV_{t.p.}$) and two-directional in-plane VE MRI (reference $PWV_{i.p.}$).

Conventional $PWV_{t.p.}$ at three aortic locations

Two non-segmented k-space sampled, one-directional through-plane VE MRI acquisitions were assessed as shown in Figure 1, B1 (First; at the level of the pulmonary trunk and second; at the abdominal aorta 10cm below the diaphragm) (9). Scan parameters: 90% rectangular field-of-view (FOV)=300×270mm^2, 8mm slice thickness, echo time (TE)=2.9ms, repetition time (TR)=4.9ms, flip angle (α)=20°, acquisition voxel size=2.3×2.1×8.0mm^3, sampling bandwidth 449Hz, number of signal averages (NSA)=2. Retrospective gating was performed with maximal number of phases reconstructed using view-sharing. The true temporal resolution (TRes, defined as 2×TR) amounted to 9.8ms. The velocity-sensitivity at the first level was set to 150cm/s and at the second level 100cm/s, respectively. Free breathing was allowed.

EPI-accelerated $PWV_{t.p}$ at five aortic locations

Four one-directional through-plane VE MRI acquisitions were assessed as shown in Figure 1, C1 (first level; aortic valve; second level; pulmonary trunk; third level; diaphragm; fourth level; just above aortic bifurcation). Scan parameters: 90% rectangular FOV=300×270 mm^2, 8mm slice thickness, TE=6.6ms, TR=12ms, α=20°, acquisition voxel

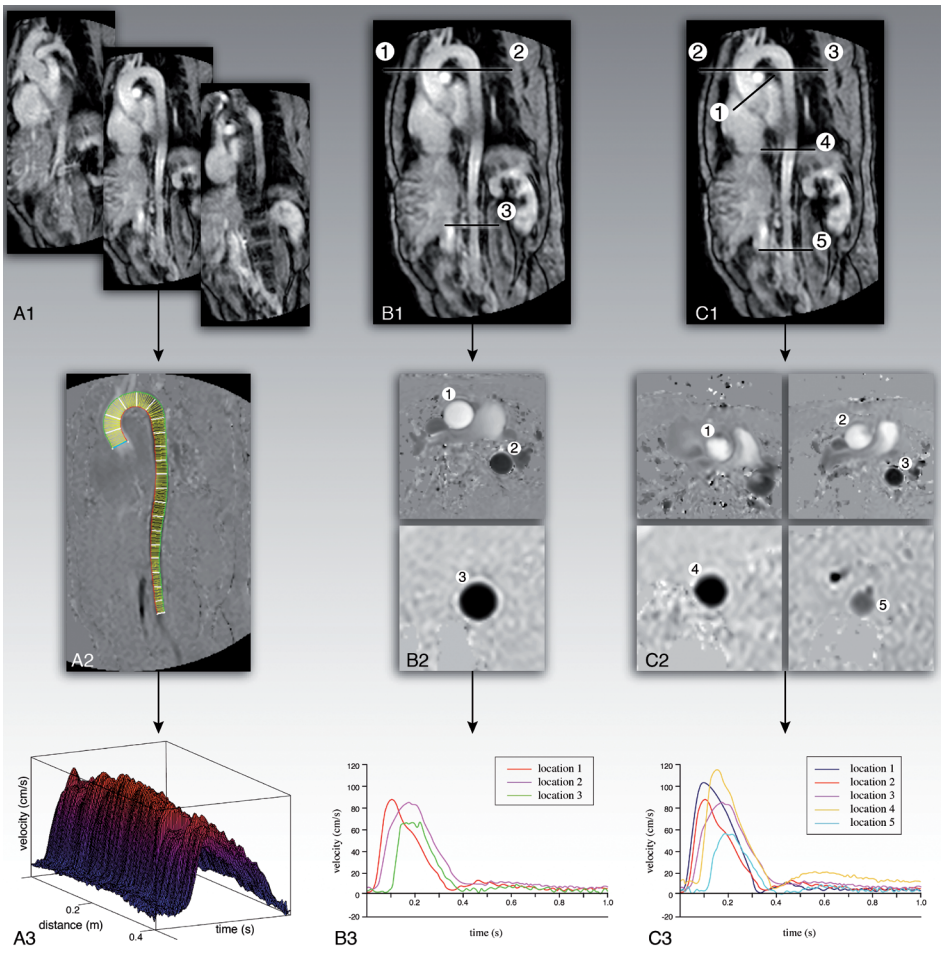

Figure 1. Representation of three methods for aortic PWV-assessment by VE MRI. (A) Reference $PWV_{i.p.}$: dense temporal and spatial sampling. Reference $PWV_{i.p.}$ was performed by means of a double-oblique stack of three consecutive slices (A1) with two-directional in-plane velocity-encoding covering the total aorta (A2). The transit-time method was used for the velocity waveforms (A3) to determine the pulse wave velocity at 200 positions along the aortic centre line.
(B) Conventional $PWV_{t.p.}$: dense temporal but sparse spatial sampling. Conventional $PWV_{t.p.}$ was performed by 2-slice through-plane velocity-encoded MRI at three aortic locations: (B1) at the level of; the ascending aorta (1), the proximal descending aorta (2) and the abdominal aorta approximately 10cm below the diaphragm (3) with the corresponding phase-velocity images (B2). From the propagation of the resulting velocity waveforms (B3), conventional $PWV_{t.p}$ is determined.
(C) EPI-accelerated $PWV_{t.p.}$: sparse temporal but improved spatial sampling. EPI-accelerated $PWV_{t.p.}$ was performed by 4-slice through-plane velocity-encoded MRI at five aortic locations: (C1) at the level of; the aortic root (1), the ascending aorta (2), the proximal descending aorta (3), the diaphragm (4) and just above the aortic bifurcation (5) with the corresponding phase-velocity images (C2). From the propagation of the resulting velocity waveforms (C3), EPI-accelerated $PWV_{t.p}$ is determined.
(Abbreviations: PWV pulse wave velocity; VE velocity-encoded; MRI magnetic resonance imaging; $PWV_{t.p}$ Pulse Wave Velocity from through-plane velocity-encoded MRI; $PWV_{i.p.}$ Pulse Wave Velocity from in-plane velocity-encoded MRI).

size=2.3×2.1×8.0mm^3, sampling bandwidth 95Hz, NSA=1. Acceleration by commercially-available EPI with EPI-factor 11 was used. This resulted in a longer TR and consequently a lower TRes (i.e., 24ms). Retrospective gating was performed with maximal number of phases reconstructed. The velocity-sensitivity for the first two acquisitions was set to 150cm/s, and for the two distal acquisitions 100cm/s. Breath-holding at end-expiration was performed for each acquisition.

Reference $PWV_{i.p.}$

Reference $PWV_{i.p}$ was assessed by two consecutive three-slice two-directional in-plane VE MRI acquisitions (Figure 1, A1) with the full aorta captured in the same volume as acquired with the 3-slice cine SSFP sequence. This method has been described and validated previously (8). In short, velocity-encoding was performed in phase-encoding and frequency-encoding direction consecutively. The velocity-sensitivity was set to 150cm/s. Scan parameters: 60% rectangular FOV=450×270mm^2, 10mm slice thickness, TE=2.4ms, TR=4.3ms, α=10°, acquisition voxel size=3.5×2.1×10.0 mm^3, sampling bandwidth 495Hz and NSA=2. Retrospective gating was performed with maximal number of phases reconstructed. TRes amounted to 8.6msec. Free breathing was required.

Image analysis

$PWV_{t.p.}$

$PWV_{t.p.}$ was determined by the transit-time method (8). The aortic path length (Δx) between subsequent sampling sites was manually determined using MASS software (Leiden University Medical Center, Leiden, The Netherlands), by placing a poly-line along the centerline of the aorta. Wave propagation was evaluated from maximal velocity-time curves that were obtained at each sampling site by using FLOW software (Leiden University Medical Center, Leiden, The Netherlands) with automated contour detection for image segmentation. The foot-to-foot definition was used for transit-time (Δt) assessment, with automated detection of the foot of the systolic velocity wave front (i.e. the wave arrival time) by detecting the intersection point of the horizontal line modeling the constant diastolic flow and a line along upslope of the systolic wave front, modeled by linear regression along 20% to 80% of the range of the flow velocity values along this upslope. PWV, defined as Δx/Δt, was determined by linear regression of the relation between sampling position and wave arrival time.

$PWV_{i.p.}$

The aorta was manually segmented from the three-slice dataset. The aortic centerline was then automatically determined and 200 equidistantly spaced sampling chords perpendicular to the centerline were defined. The velocity in the direction parallel to the centerline was constructed from the two acquired velocity components. The aortic flow velocity was sampled along each chord to define the maximal velocity per chord. For each chord and each phase, the maximal velocity value over the three slices was

determined (i.e., maximal-velocity-projection), resulting in 200 maximal velocity waveforms. The position along the aortic centerline was determined from a manually traced poly-line in the slab of the three para-sagittal slices. The arrival time of each of the 200 waveforms at their corresponding positions along the aortic centerline was automatically determined similarly as for $PWV_{t.p.}$-assessment.

Statistical analysis

Image analysis was performed by one observer (in a blinded manner) with more than 15 years experience in cardiac MRI. Conventional $PWV_{t.p.}$ was compared to EPI-accelerated $PWV_{t.p.}$ against the reference $PWV_{i.p.}$, both for the total aorta and for the aortic arch. Continuous variables are expressed as mean ± standard deviation (SD). Mean signed and unsigned differences and 95%-confidence interval (95%-CI) were determined for paired variables and the statistical significance of these differences were evaluated using paired t-tests. A significance level $p<0.05$ was used. The coefficient of variation (COV), defined as the SD of the differences divided by the mean of both measurements, was determined to express variation between measurements. Bland-Altman plots were determined to study systematic differences. Correlation between variables was tested by Pearson correlation coefficient (r). Statistical significance of the difference between correlation coefficients for conventional and accelerated $PWV_{t.p.}$ versus $PWV_{i.p.}$ was tested by stepwise linear regression analysis with $PWV_{t.p.}$ as dependent variable and $PWV_{i.p.}$ and the interaction between $PWV_{i.p.}$ and conventional versus accelerated $PWV_{t.p.}$ as predictors. All statistical analyses were performed using PASW Statistics version 17.0.2 (SPSS, Chicago, IL).

RESULTS

Table 1 summarizes mean heart rate and scan times for all three PWV-methods. The mean length of the evaluated total aorta was 32±4cm and mean length of the evaluated aortic arch was 12±3cm.

Table 1. Heart rate and scan times for the three methods for PWV-assessment.

	Heart rate* (bpm)	Total scan time* (minutes)	Scan time per slice* (seconds)
Reference $PWV_{i.p.}$	66 ± 10	14 ± 2	NA
Conventional $PWV_{t.p.}$	67 ± 10	7 ± 1	214 ± 34
EPI-accelerated $PWV_{t.p.}$	66 ± 9	1 ± 0.2	17 ± 2

*Data are represented as mean ± standard deviation.
Abbreviations: NA: not applicable; $PWV_{i.p.}$: Pulse Wave Velocity from in-plane velocity-encoded MRI; $PWV_{t.p.}$: Pulse Wave Velocity from through-plane velocity-encoded MRI

Total Aorta

PWV results for the total aorta are presented in Bland-Altman plots, including limits of agreement (Figure 2, A-B). No obvious trends in the differences were observed. Statistical results are presented in Table 2. EPI-accelerated $PWV_{t.p.}$ showed a significantly stronger correlation (p=0.03) with reference $PWV_{i.p}$ than conventional $PWV_{t.p.}$ (r=0.92, p<0.001 versus r=0.65, p=0.001, respectively). Furthermore, as illustrated in the Bland-Altman plot as well as expressed in COV, the variation with reference $PWV_{i.p.}$ is lower for EPI-accelerated $PWV_{t.p.}$ than for conventional $PWV_{t.p.}$ (COV=11% versus COV=27%, respectively). There was no significant difference for either $PWV_{t.p.}$-method when compared with reference $PWV_{i.p.}$ but the unsigned error for EPI-accelerated $PWV_{t.p.}$ amounted to 8% while 16% for conventional $PWV_{t.p.}$. Of note, 84% scan time reduction was achieved for EPI-accelerated $PWV_{t.p.}$ when compared to conventional $PWV_{t.p.}$ (1 minute versus 7 minutes).

Table 2. Conventional $PWV_{t.p.}$ and EPI-accelerated $PWV_{t.p.}$ versus reference $PWV_{i.p.}$

	Total Aorta		Aortic Arch	
	conventional $PWV_{t.p.}$	EPI-accelerated $PWV_{t.p.}$	conventional $PWV_{t.p.}$	EPI-accelerated $PWV_{t.p.}$
Pearson r	0.65	0.92	0.67	0.66
Difference (m/s)*	0.05±1.68	0.19±0.63	-0.53±1.36	-0.20±1.63
p-value t-test	0.88	0.16	0.07	0.57
Mean unsigned error	16%	8%	18%	21%
Coefficient of variation	27%	11%	24%	28%
Total scan time (seconds)*	428±68	68±10	214±34	17±2

*Data are represented as mean ± standard deviation.
Abbreviations: $PWV_{i.p.}$: Pulse Wave Velocity from in-plane velocity-encoded MRI; $PWV_{t.p.}$: Pulse Wave Velocity from through-plane velocity-encoded MRI.

Aortic Arch

PWV results for regional assessment in the aortic arch are presented in Bland-Altman plots (Figure 2, C-D). No obvious trends in the differences were observed. Statistical results are presented in Table 2. Agreement for both $PWV_{t.p.}$-methods against $PWV_{i.p}$ was not significantly different (p=0.46; conventional $PWV_{t.p.}$: r=0.67, p<0.001; EPI-accelerated $PWV_{t.p.}$: r=0.66, p=0.001). Also the variation with reference $PWV_{i.p}$ was comparable for both conventional $PWV_{t.p.}$ and EPI-accelerated $PWV_{t.p.}$ (COV=24% versus COV=28%, respectively). No significant difference for either $PWV_{t.p.}$-method was present when compared with reference $PWV_{i.p.}$ and unsigned errors were comparable (18% versus 21%, respectively). Of note, 92% scan time reduction was achieved for EPI-accelerated $PWV_{t.p}$ when compared to conventional $PWV_{t.p}$ (17 seconds versus 4 minutes).

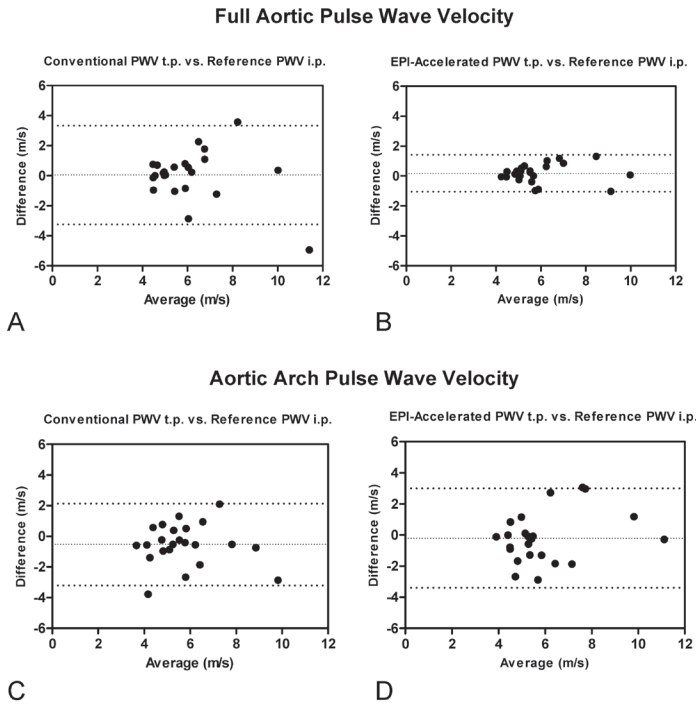

Figure 2. Conventional $PWV_{t.p.}$ and EPI-accelerated $PWV_{t.p.}$ versus reference $PWV_{i.p.}$, both globally for the total aorta (**A,B**) and regionally for the aortic arch (**C,D**). The dashed lines represent the limits of agreement. (Abbreviations: $PWV_{t.p.}$ Pulse Wave Velocity from through-plane velocity-encoded MRI; $PWV_{i.p.}$ Pulse Wave Velocity from in-plane velocity-encoded MRI).

DISCUSSION

In this study, the effect of temporal and spatial sampling density on aortic PWV-assessment was evaluated. The main findings are: 1) For global PWV-assessment in the total aorta, EPI-accelerated $PWV_{t.p.}$ with improved spatial sampling at five aortic locations is more accurate than conventional $PWV_{t.p.}$ with sampling at three aortic locations, despite inferior temporal resolution due to EPI-acceleration; 2) For regional PWV-assessment in the aortic arch, EPI-accelerated $PWV_{t.p.}$ is comparable to conventional $PWV_{t.p.}$ with respect to accuracy and variation. Because of the additional 92% scan time reduction, EPI-accelerated $PWV_{t.p.}$ is preferred over conventional $PWV_{t.p.}$.

It has been reported that dense temporal and spatial PWV-sampling with in-plane VE MRI (in our study used as the standard of reference $PWV_{i.p.}$) showed higher agreement with invasive pressure measurements, the gold standard for PWV-assessment, and higher reproducibility when compared to conventional $PWV_{t.p.}$ (6). However, $PWV_{i.p.}$-sampling is time-consuming as acquisition time typically amounts to 15 minutes. Furthermore, image analysis is more elaborate for $PWV_{i.p.}$-assessment. Therefore, estimations of global

and regional aortic PWV are usually obtained from multi-slice through-plane VE MRI, with the number of acquisition planes along the aorta defining spatial sampling density. Adding acquisition planes along the aorta increases spatial sampling density, but also adds to the total scan time. Applying multiple readouts for a single echo will accelerate scan time but at the cost of decreasing temporal sampling resolution. To our knowledge, the effect of temporal and spatial sampling density on aortic PWV-assessment with VE MRI has not been evaluated yet. In our study, the effect of temporal sampling density is evaluated by comparing single-echo readout with EPI-accelerated multi-echo readout. Conventional $PWV_{t.p.}$ showed moderate correlation (r=0.65) with the reference $PWV_{i.p.}$, considerable varation (COV=27%) and a mean unsigned error of 16%. Despite inferior temporal resolution (TRes=24ms instead of TRes=9.8ms), improving spatial sampling density by adding two aortic sampling locations significantly (p=0.03) improved correlation with reference $PWV_{i.p.}$ (r=0.92) and lowered both variation (COV=11%) and mean unsigned error (8%). Additionally, EPI-accelerated $PWV_{t.p.}$ at five aortic locations also resulted in 84% scan time reduction.

In patients with MFS as well as other cardiovascular diseases with regional manifestation of impaired aortic wall stiffening, PWV-assessment at a regional level is of high interest (3). Temporal sampling resolution is a potentially limiting factor defining accuracy of regional PWV-assessment. However, the present study showed that EPI-accelerated $PWV_{t.p.}$-sampling is in comparable good agreement with reference $PWV_{i.p.}$ as conventional $PWV_{t.p.}$-sampling, despite almost 2.5-fold inferior temporal sampling resolution. EPI-accelerated $PWV_{t.p.}$-sampling is still advantageous for regional PWV-assessment since it accounts for 92% scan time reduction.

The following limitations need to be acknowledged. This study is a retrospective analysis in a relative small study population. In our study, only MFS patients were investigated and not other patient groups or healthy volunteers. However, regional PWV-assessment is of high interest particularly in this patient population, as PWV-values in the proximal aorta are expected to be increased. Furthermore, the use of EPI-acceleration is another limitation, as it will result in significant errors in velocity values (11). On the other hand, these errors will have minimal influence on PWV-assessment, as this only relies on the ability to assess the transit-time from velocity waveforms and not on accurate velocity assessment. Other acceleration strategies such as parallel imaging or k-t blast can be potentially useful to accelerate acquisition even further (12,13). In addition, breath-holding was performed only during EPI-accelerated $PWV_{t.p.}$-assessment. A previous study by Ley et al. demonstrated the effect of different breathing maneuvers during MRI acquisitions on hemodynamics (14). Since we have not performed a comparison between different breathing maneuvers on PWV measurements, a potential effect of free-breathing versus breath-holding on different PWV-assessments could not be excluded. In this study, only scan time was reported and compared for different PWV-assessments. It should be noted that for positioning additional imaging planes additional examination time is required and depends on the experience of the MRI technician. On the other hand, planning additional acquisition planes can usually be performed during scan time of

previous acquisition series and therefore no additional examination time should be required. Finally, for comparison of global aortic $PWV_{t.p.}$-assessment, not identical aortic trajectories were compared. The five aortic sample locations (for EPI-accelerated $PWV_{t.p.}$-assessment) encompassed the aortic trajectory from aortic valve to bifurcation, while conventional $PWV_{t.p.}$-assessment was sampled from ascending aorta to the level 10cm below the diaphragm. For both $PWV_{t.p.}$-assessments, the corresponding aortic trajectory of the reference $PWV_{i.p.}$-assessment was matched for comparison. Furthermore, regional PWV was evaluated in identical aortic trajectory.

In conclusion, this study evaluated the effect of temporal and spatial sampling density on PWV-assessment globally in the total aorta and regionally in the aortic arch in patients with MFS using through-plane velocity-encoded MRI. Improving spatial sampling density by adding two acquisition planes along the aorta resulted in more accurate PWV-assessment, even when temporal resolution decreased 2.5-fold by EPI-acceleration. For regional PWV-assessment, EPI-accelerated and conventional PWV-assessment are comparable accurate. Scan time reduction makes EPI-accelerated PWV-assessment the preferred method-of-choice.

REFERENCES

1. Yetman AT, Graham T. The dilated aorta in patients with congenital cardiac defects. J Am Coll Cardiol 2009;53:461-467.
2. Nollen GJ, Groenink M, Tijssen JG, van der Wall EE, Mulder BJ. Aortic stiffness and diameter predict progressive aortic dilatation in patients with Marfan syndrome. Eur Heart J 2004;25:1146-1152.
3. Cavalcante JL, Lima JA, Redheuil A, Al-Mallah MH. Aortic stiffness current understanding and future directions. J Am Coll Cardiol 2011;57:1511-1522.
4. Vlachopoulos C, Aznaouridis K, Stefanadis C. Prediction of cardiovascular events and all-cause mortality with arterial stiffness: a systematic review and meta-analysis. J Am Coll Cardiol 2010;55:1318-1327.
5. Forteza A, Evangelista A, Sanchez V et al. [Study of the efficacy and safety of losartan versus atenolol for aortic dilation in patients with Marfan syndrome]. Rev Esp Cardiol 2011;64:492-498.
6. Ahimastos AA, Aggarwal A, D'Orsa KM et al. Effect of perindopril on large artery stiffness and aortic root diameter in patients with Marfan syndrome: a randomized controlled trial. JAMA 2007;298:1539-1547.
7. Westenberg JJ, Scholte AJ, Vaskova Z et al. Age-related and regional changes of aortic stiffness in the marfan syndrome: Assessment with velocity-encoded MRI. J Magn Reson Imaging 2011;34:526-531.
8. Westenberg JJ, de Roos A, Grotenhuis HB et al. Improved aortic pulse wave velocity assessment from multislice two-directional in-plane velocity-encoded magnetic resonance imaging. J Magn Reson Imaging 2010;32:1086-1094.
9. Grotenhuis HB, Westenberg JJ, Steendijk P et al. Validation and reproducibility of aortic pulse wave velocity as assessed with velocity-encoded MRI. J Magn Reson Imaging 2009;30:521-526.
10. de Paepe A, Devereux RB, Dietz HC, Hennekam RC, Pyeritz RE. Revised diagnostic criteria for the Marfan syndrome. Am J Med Genet 1996;62:417-426.
11. Zaitsev M, Hennig J, Speck O. Point spread function mapping with parallel imaging techniques and high acceleration factors: fast, robust, and flexible method for echo-planar imaging distortion correction. Magn Reson Med 2004;52:1156-1166.
12. Niendorf T, Sodickson DK. Parallel imaging in cardiovascular MRI: methods and applications. NMR Biomed 2006;19:325-341.
13. Beerbaum P, Korperich H, Gieseke J, Barth P, Peuster M, Meyer H. Blood flow quantification in adults by phase-contrast MRI combined with SENSE—a validation study. J Cardiovasc Magn Reson 2005;7:361-369.
14. Ley S, Fink C, Puderbach M et al. MRI Measurement of the hemodynamics of the pulmonary and systemic arterial circulation: influence of breathing maneuvers. AJR Am J Roentgenol 2006;187:439-444.